IEEE Std 115A-1987
(Supplement to ANSI/IEEE Std 115-1983)
(Revision of IEEE Std 115A, originally
issued for trial use in 1984)

IEEE Standard Procedures for Obtaining Synchronous Machine Parameters by Standstill Frequency Response Testing

(Supplement to ANSI/IEEE Std 115-1983)

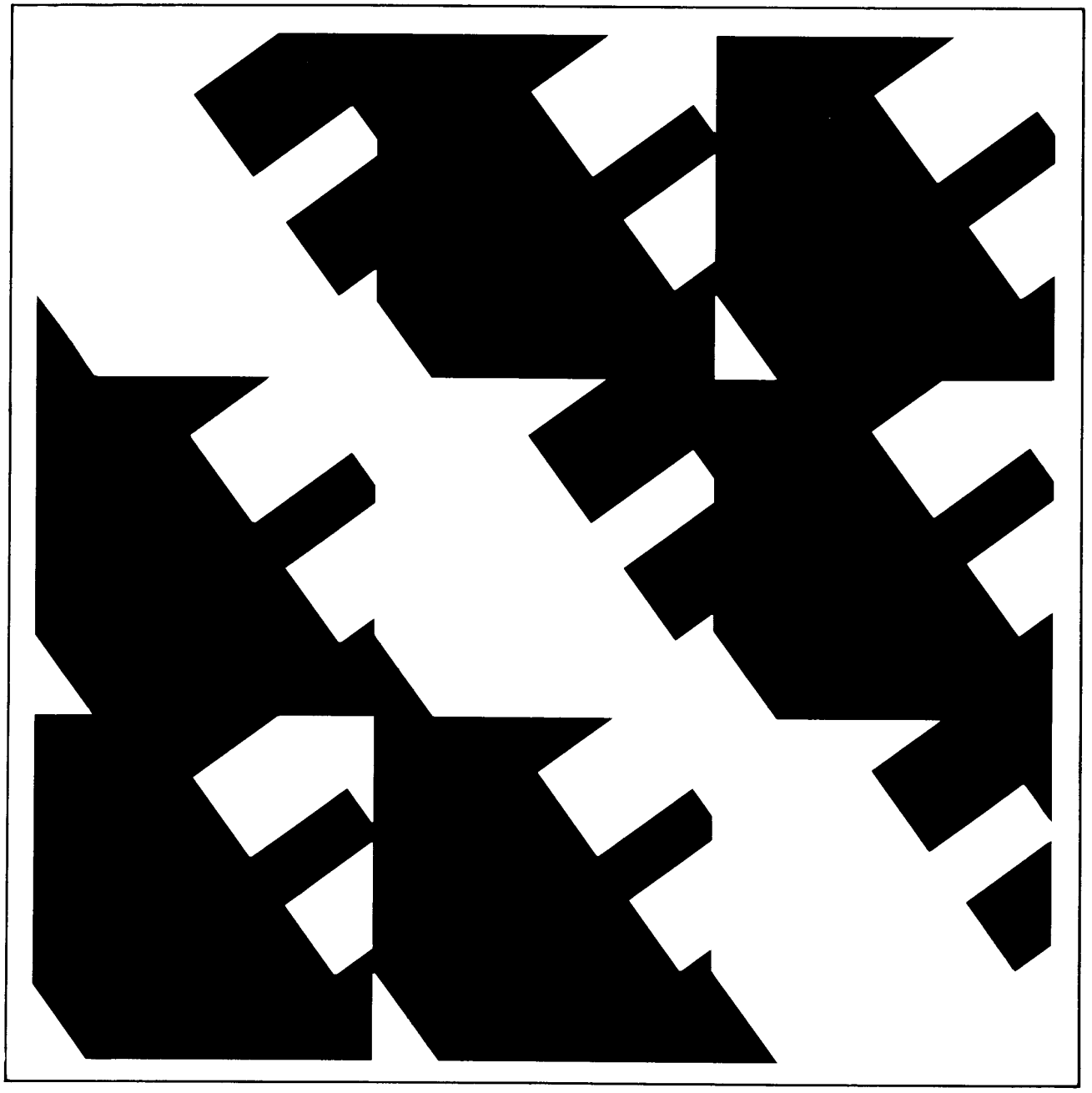

IEEE Std 115A-1987

Published by The Institute of Electrical and Electronics Engineers, Inc 345 East 47th Street, New York, NY 10017, USA
May 18, 1987
SH11221

IEEE
Std 115A-1987

(Supplement to
ANSI/IEEE Std 115-1983)

(Revision of
IEEE Std 115A,
originally issued
for trial use in 1984)

IEEE Standard Procedures for Obtaining Synchronous Machine Parameters by Standstill Frequency Response Testing

(Supplement to ANSI/IEEE Std 115-1983, IEEE Guide: Test Procedures for Synchronous Machines)

Sponsor

Power System Engineering Committee
and the
Rotating Machinery Committee
of the
IEEE Power Engineering Society

The Institute of Electrical and Electronics Engineers, Inc
345 East 47th Street, New York, NY 10017, USA

IEEE Standards documents are developed within the Technical Committees of the IEEE Societies and the Standards Coordinating Committees of the IEEE Standards Board. Members of the committees serve voluntarily and without compensation. They are not necessarily members of the Institute. The standards developed within IEEE represent a consensus of the broad expertise on the subject within the Institute as well as those activities outside of IEEE which have expressed an interest in participating in the development of the standard.

Use of an IEEE Standard is wholly voluntary. The existence of an IEEE Standard does not imply that there are no other ways to produce, test, measure, purchase, market, or provide other goods and services related to the scope of the IEEE Standard. Futhermore, the viewpoint expressed at the time a standard is approved and issued is subject to change brought about through developments in the state of the art and comments received from users of the standard. Every IEEE Standard is subjected to review at least once every five years for revision or reaffirmation. When a document is more than five years old, and has not been reaffirmed, it is reasonable to conclude that its contents, although still of some value, do not wholly reflect the present state of the art. Users are cautioned to check to determine that they have the latest edition of any IEEE Standard.

Comments for revision of IEEE Standards are welcome from any interested party, regardless of membership affiliation with IEEE. Suggestions for changes in documents should be in the form of a proposed change of text, together with appropriate supporting comments.

Interpretations: Occasionally questions may arise regarding the meaning of portions of standards as they relate to specific applications. When the need for interpretations is brought to the attention of IEEE, the Institute will initiate action to prepare appropriate responses. Since IEEE Standards represent a consensus of all concerned interests, it is important to ensure that any interpretation has also received the concurrence of a balance of interests. For this reason IEEE and the members of its technical committees are not able to provide an instant response to interpretation requests except in those cases where the matter has previously received formal consideration.

Comments on standards and requests for interpretations should be addressed to:

Secretary, IEEE Standards Board
345 East 47th Street
New York, NY 10017
USA

Foreword

(This Foreword is not a part of IEEE Std 115A-1987, IEEE Standard Procedures for Obtaining Synchronous Machine Parameters by Standstill Frequency Response Testing.)

This document is the result of work undertaken by the Task Force on Definitions and Procedures, which was formed in 1978 by the Joint Working Group on Determination and Application of Synchronous Machine Models for Stability Studies. The Joint Working Group was itself constituted in 1973 by the Power System Engineering Committee and Rotating Machinery Committee. The working group reported to the Computer and Analytical Methods Subcommittee of the PSE Committee and the Synchronous Machinery Subcommittee of the Rotating Machinery Committee.

The initial thrust of their work could be construed as power system oriented, since the need for higher order stability models, principally for turbogenerators, became apparent as power system analysis began applying static excitation systems and supplementary excitation controls in order to improve stability. With this application came the need for improved computer simulations and the corresponding need for better stability data.

A milestone in the development of this work was the publication, by the Task Force of the Joint Working Group, of "Supplementary Definitions and Associated Test Methods for Obtaining Parameters for Synchronous Machine Stability Study Simulations" in the *IEEE Transactions on Power Apparatus and Systems*, July/August 1980. Thus the need to produce an IEEE standard on the new, recommended procedures, which involved frequency response testing, was apparent to the Joint Working Group. They recommended that the Task Force on Definitions and Procedures address this problem.

The first draft of the current document was transmitted by our Task Force in 1981 to a Working Group of the Synchronous Machinery Subcommittee. This working group, under the chairmanship of Paul I. Nippes, was reviewing IEEE Std 115-1965. Paul G. Cummings, liaison from the Rotating Machinery Committee to the Standards Board, recommended that the Trial Procedure be considered for the present as a supplement to the new ANSI/IEEE Std 115-1983, and hence it was designated IEEE Std 115A. It is presently proposed, when ANSI/IEEE Std 115 is again a candidate for revision, that IEEE Std 115A-1987 will become an integral part of it.

The Task Force and the Joint Working Group wish to acknowledge the assistance of Paul I. Nippes and his working group associates. J. C. White, as Chairman of the Synchronous Machinery Subcommittee during the initial submission of this document, was instrumental in expediting the approval process by the Rotating Machinery Committee. Carl Flick, current Chairman of the Synchronous Machinery Subcommittee, also helped materially, as did Paul G. Cummings, who was of considerable assistance during the Standards Board review process.

Many more names could be mentioned in this Foreword. The entire Task Force on Definitions and Procedures participated in the preparation of the first draft of this document, but special thanks should go to Wilfred Watson and Murray E. Coultes of Ontario Hydro for their comments and encouragement during the initial formulation, between 1979 and 1982, of the ideas presented in the following pages.

At the time this standard was initially approved, the Special Task Force on Definitions and Procedures had the following membership:

Paul L. Dandeno, *Chairman*

Daniel H. Baker	L. N. Hannett	H. Reid Schwenk
Murray E. Coultes	S. J. Salon	Stephen Umans

At the time this standard was initially approved, the members of the working group of the Synchronous Machinery Subcommittee were:

Paul I. Nippes, *Chairman*

Paul G. Cummings	William R. McCown	Stephen Umans
Karl F. Drexler	Joseph V. Pospisil	Joseph J. Wilkes

At the time this standard was affirmed and approved, the Power System Engineering and Rotating Machinery Committees' Group on Determination and Application of Synchronous Machine Models for Stability Studies of the IEEE Power Engineering Society had the following membership:

Paul L. Dandeno, *Chairman*

Paul M. Anderson
Daniel H. Baker
George Buckley
F. Paul De Mello
Raymond D. Dunlop
James Edmonds
John Fowler
L. N. Hannett
Steven Herling
David C. Lee
Stephen Minnich
S. J. Salon
H. Reid Schwenk
Geoffrey Shackshaft
Stephen Umans

The following persons were on the balloting committee that approved this document for submission to the IEEE Standards Board:

P. D. Agarwall
J. C. Andreas
R. H. Auerbach
R. G. Bartheld
T. H. Barton
L. W. Buchanan
G. W. Buckley
A. W. W. Cameron
M. V. K. Chari
J. L. Cohon
J. L. Craggs
P. G. Cummings
N. A. Demerdash
W. C. Dumper
J. S. Edmonds
J. S. Ewing
C. Flick
N. K. Ghai
D. R. Green
F. H. Grooms
H. B. Hamilton
G. E. Herzog
G. W. Herzog
M. H. Hesse
T. J. Higgins
V. B. Honsinger
R. F. Horrell
W. D. Jones
H. E. Jordan
E. I. King
W. H. Koch
P. R. H. Landrieu
T. A. Lipo
T. J. Lorenz
H. Majmudar
W. J. Martiny
C. H. Merrifield
E. J. Michaels
R. C. Moore
E. H. Myers
N. E. Nilsson
P. I. Nippes
D. W. Novotny
J. L. Oldenkamp
J. A. Oliver
W. B. Penn
M. Poloujadoff
J. V. Pospisil
E. P. Priebe
G. M. Rosenberry
C. M. Rowe
M. S. Sarma
P. W. Sauer
R. M. Saunders
P. T. Schuerman
D. K. Sharma
M. W. Sheets
W. J. Sheets
E. P. Smith
J. F. Szablya
P. H. Trickey
P. J. Tsivitse
J. P. Voglewede
P. Walker
T. C. Wang
R. F. Weddleton
J. C. White
E. C. Whitney
J. J. Wilkes
E. J. Woods

When the IEEE Standards Board approved this standard on December 11, 1986, it had the following membership:

John E. May, *Chairman*

Irving Kolodny, *Vice Chairman*

Sava I. Sherr, *Secretary*

James H. Beall
Fletcher J. Buckley
Paul G. Cummings
Donald C. Fleckenstein
Jay Forster
Daniel L. Goldberg
Kenneth D. Hendrix
Irvin N. Howell
Jack Kinn
Joseph L. Koepfinger*
Edward Lohse
Lawrence V. McCall
Donald T. Michael*
Marco W. Migliaro
Stanley Owens
John P. Riganati
Frank L. Rose
Robert E. Rountree
Martha Sloan
Oley Wanaselja
J. Richard Weger
William B. Wilkens
Helen M. Wood
Charles J. Wylie
Donald W. Zipse

*Member Emeritus

Contents

APPENDIX FIGURES PAGE

IEEE Standard Procedures for Obtaining Synchronous Machine Parameters by Standstill Frequency Response Testing

1. Introduction

In Section 8 of ANSI/IEEE Std 115-1983 [1][1], methods are described for obtaining synchronous machine parameters in the form of reactances and time constants. These are the familiar synchronous, transient and subtransient reactances as well as open-circuit and short-circuit, transient and subtransient time constants.

Three reactances and two time constants have historically been determined from the test data resulting from the procedures outlined in Section 8 of ANSI/IEEE Std 115-1983 [1]. Accordingly, it has been customary to assume a two-rotor-circuit direct-axis model to describe the synchronous machine mathematically in stability and other related analyses. Figure 1 shows the corresponding equivalent circuit; the Laplace transform analysis of this circuit is detailed in [7].

The assumed quadrature-axis equivalent circuit is similar in structure, except that the field winding is replaced by a second (equivalent) iron circuit.

Accurate identification of the field circuit is a desirable feature for present day stability analyses where excitation controls play an important role. This is not possible with the tests described in Section 8 of ANSI/IEEE Std 115-1983 [1].

Another difficulty with ANSI/IEEE Std 115-1983 [1] lies in defining adequate tests for quadrature-axis quantities. Test procedures, described in 8.5, are available for determining quadrature-axis synchronous reactances. There are no practical or acceptable procedures listed in Section 8 for obtaining quadrature-axis transient or subtransient reactances or time constants. Present day stability studies require quadrature-axis as well as direct-axis values for an accurate and adequate synchronous machine stability simulation.

A new approach has demonstrated that stability parameters for synchronous machines can be obtained by performing frequency response tests with the machine at standstill. Frequency response data describe the response of machine fluxes to stator current and field voltage changes in both the direct and quadrature axes of a synchronous machine. Some advantages of the method are that it can be done either in the factory or on site, it poses a low probability of risk to the machine being tested, and it provides complete data in both direct and quadrature axes. Resistances and reactances for the associated models can be calculated using the methods in the Appendix.

The model parameters derived from the standstill frequency response tests reflect linearized conditions, with extremely low flux conditions in

Fig 1
Conventional *d*-Axis Equivalent Circuit

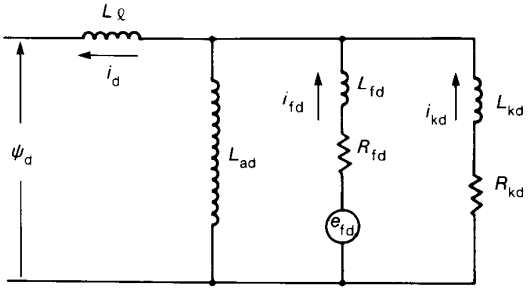

L_ℓ = armature leakage inductance
L_{fd} = field leakage inductance
L_{kd} = direct-axis rotor equivalent leakage inductance
L_{ad} = stator to rotor mutual inductance
R_{fd} = field resistance
R_{kd} = direct-axis rotor equivalent resistance

[1] The numbers in brackets correspond to those of the references listed in Section 2 of this standard.

the machine. The values of L_{ad} and L_{aq} obtained from the test data must each be adjusted slightly to values corresponding to unsaturated air-gap line flux levels. This is described in Section A4 of the Appendix. Further discussion on the basis for such corrections is also given in a recent paper by Minnich [8]. Saturation may then be treated in stability simulations in a conventional manner by adjusting L_{ad} and L_{aq}. The usefulness of the models obtained according to these procedures has been demonstrated by comparing on-site power system test disturbances, associated with line openings or closings, with computer simulations. The responses of cylindrical rotor machines were investigated in this limited number of tests. This standard provides a means of gaining further experience with the circumstances by which turbogenerator models, in particular, based on standstill frequency response testing, can be used for power system stability studies or other applications such as excitation control analyses.

Users of this test method compared the simulated performance of the standstill models with actual generator or system responses under loaded conditions. In some instances it is very possible that on-line or open-circuit rated-speed frequency response testing or line switching tests are needed either to confirm the validity of the standstill models, or to adjust them to reflect loaded conditions at rated speed. (Refer to [3].) The effect of centrifugal forces on slot wedge characteristics in cylindrical rotor machines is one example of possible electrical or magnetic rotor circuit changes under operating loaded conditions, as is the effect of saturation in both the direct and quadrature axes.

Aspects of standstill frequency response testing that are different from the procedures in Section 8 of ANSI/IEEE Std 115-1983 [1] are the measurement accuracy requirements and the complexity of the data reduction techniques. Instrumentation capable of resolving magnitudes and phase angles of fundamental components of ac signals at low frequencies (possibly down to 0.001 Hz) is required. In addition, the procedure for translating the test data into synchronous machine stability study constants requires a computerized, curve-fitting technique. An illustrative example is shown in the Appendix.

The following sections describe the application of standstill frequency response testing methods for obtaining direct- and quadrature-axis stability parameters. Some of the basic work performed in this area is described in [2], [3], [4], [5], and [6].

2. References

The following publications shall be used in conjunction with this standard:

[1] ANSI/IEEE Std 115-1983, IEEE Guide: Test Procedures for Synchronous Machines.[2]

[2] COULTES, M. E. and WATSON, W. Synchronous Machine Models by Standstill Frequency Response Tests. *IEEE Transactions on Power Apparatus and Systems*, vol PAS-100, no 4, Apr 1981, pp 1480-1489.

[3] DANDENO, P. L., KUNDUR, P., PORAY, A. T. and ZEIN EL-DIN, H. M. Adaption and Validation of Turbogenerator Model Parameters Through On-Line Frequency Response Measurements. *IEEE Transactions on Power Apparatus and Systems*, vol PAS-100, no 4, Apr 1981, pp 1658-1664.

[4] DANDENO, P. L., KUNDUR, P., PORAY, A. T. and COULTES, M.E. Validation of Turbogenerator Stability Models by Comparison with Power System Tests. *IEEE Transactions on Power Apparatus and Systems*, vol PAS-100, no 4, Apr 1981, pp 1637-1645.

[5] Determination of Synchronous Machine Stability Study Constants. EPRI Report EL 1424: vol 1, Sept 1980, Westinghouse Electric Corporation, and vol 2, Dec 1980, Ontario Hydro (two of four reports on EPRI Project 997).

[6] HURLEY, J. D. and SCHWENK, H. R. Standstill Frequency Response Modeling and Evaluation by Field Tests on a 645 MVA Turbine Generator. *IEEE Transactions on Power Apparatus and Systems*, vol PAS-100, no 2, Feb 1981, pp 828-836.

[7] IEEE Joint Working Group on Determination of Synchronous Machine Stability Constants—Supplementary Definitions and Associated Test Methods for Obtaining Parameters for Synchronous Machine Stability Study Simulations. *IEEE Transactions on Power Apparatus and Systems*, vol PAS-99, no 4, Jul/Aug 1980, pp 1625-1633.

[8] MINNICH, S. H. Small Signals, Large Signals and Saturation in Generator Modeling. *IEEE Transactions on Energy Conversion*, vol EC-1, Mar 1986, pp 94-102.

[2] ANSI/IEEE publications can be obtained from the Sales Department, American National Standards Institute, 1430 Broadway, New York, NY 10018, or from the Institute of Electrical and Electronics Engineers, Service Center, Piscataway, NJ 08854.

3. Definitions

The definitions below are the principal ones that power system analysts have found convenient when describing the response of synchronous machines. Although they have been published in [7], they are repeated here for completeness. The d-axis conventions are shown in the preceding Fig 1; the q-axis is similar.

$L_d(s)$ The direct-axis operational inductance. It is the ratio of the Laplace transform of the direct-axis armature flux linkages to the Laplace transform of the direct-axis current, with the field winding short-circuited.

$L_q(s)$ The quadrature-axis operational inductance. It is the ratio of the Laplace transform of the quadrature-axis armature flux linkages to the Laplace transform of the quadrature-axis current.

$G(s)$ The armature to field transfer function. It is the ratio of the Laplace transform of the direct-axis armature flux linkages to the Laplace transform of the field voltage, with the armature open-circuited.

4. Measurable Parameters at Standstill

4.1 General. The above quantities can be obtained from other measurable parameters with the machine at standstill. Early workers who investigated the concepts of rotating machine operational impedances, and by implication, operational inductances included Park, Kron, Concordia, Adkins, and others.

The three principal parameters noted below relate to the three definitions previously listed.

$Z_d(s)$ The direct-axis operational impedance is equal to $R_a + sL_d(s)$, where R_a is the relevant armature resistance per phase. The dc value is used because it is measurable, and, as will be seen in the example in the Appendix, its contribution to the total impedance is only significant at low frequencies. Also,

$$Z_d(s) = -\frac{\Delta e_d(s)}{\Delta i_d(s)}\bigg|_{\Delta e_{fd} = 0} \quad \text{(Eq 1)}$$

$Z_q(s)$ The quadrature-axis operational impedance is equal to $R_a + sL_q(s)$, where R_a is the dc armature resistance phase. Also,

$$Z_q(s) = -\frac{\Delta e_q(s)}{\Delta i_q(s)} \quad \text{(Eq 2)}$$

The above two quantities are the armature driving point impedances.

A third quantity is given by the relation

$$G(s) = \frac{\Delta e_d(s)}{s\Delta e_{fd}(s)}\bigg|_{\Delta_{id} = 0} \quad \text{(Eq 3)}$$

An alternative method of measuring this parameter is suggested as follows:

$$sG(s) = \frac{\Delta i_{fd}(s)}{\Delta i_d(s)}\bigg|_{\Delta_{efd} = 0} \quad \text{(Eq 4)}$$

The advantage of the latter form is that it can be measured at the same time as $Z_d(s)$.

A fourth measurable parameter at standstill is the armature to field transfer impedance:

$$Z_{afo}(s) = -\frac{\Delta e_{fd}(s)}{\Delta i_d(s)}\bigg|_{\Delta_{ifd} = 0} \quad \text{(Eq 5)}$$

4.2 Machine Conditions for Standstill Frequency Response Tests. The machine must be shut down, off-turning gear, and electrically isolated. The unit transformer must be disconnected from the armature terminals and any armature winding grounds removed. Also, all connections to the field terminals must be taken off. This can be done by removing the brushgear or, in the case of a brushless exciter, electrically disconnecting the complete exciter from the generator field winding.

It is important to maintain the armature winding temperature constant during the measurements since the low-frequency test points are very sensitive to the armature resistance. To this end, the machine should be cooled as close to ambient temperature as possible, and any stator heat exchangers should be turned off. Circulation of the water through the stator winding should be maintained to ensure that stagnation does not cause the water conductivity to change.

It should be possible to turn the machine rotor to a precise position prior to the tests. This is most easily done by hand cranking the turning gear. If this is not possible, a hydraulic jack can be used against a coupling bolt. Although a gantry crane may be helpful in making large movements, it is not precise enough for the final positioning of the shaft.

4.3 Required Measurements. The magnitude and phase of the desired quantities,

$$Z_d(s),\ Z_q(s),\ \text{and}\ \frac{\Delta i_{fd}(s)}{\Delta i_d(s)}$$

are measured over a range of frequencies. The minimum frequency (f_{min}) should be at least one order of magnitude less than that corresponding to the transient open-circuit time constant of the generator, that is,

$$f_{min} \simeq \frac{0.016}{T'_{do}} \quad \text{(Eq 6)}$$

The maximum frequency for the test should be somewhat greater than twice the rated frequency of the generator being tested, perhaps 200 Hz for a 60 Hz machine. Approximately 10 test points, logarithmically spaced, per decade of frequency, is a satisfactory measurement density.

The mutual inductance between the field and armature windings, L_{afd}, shall also be measured, where

$$L_{afd} = \lim_{s \to 0} \left[\left(\frac{1}{s} \right) Z_{afo}(s) \right] \quad \text{(Eq 7)}$$

The most direct way is to obtain the magnitude of the low-frequency asymptote of the transfer function $\Delta e_{fd}(s)/\Delta i_d(s)$, measured during the direct-axis tests with the field open. Alternatively, it can be calculated by multiplying the low-frequency asymptote of the magnitude of $\Delta i_{fd}(s)/\Delta i_d(s)$ by r_{fd}. r_{fd} is the total resistance in the field winding circuit during the measurement of $\Delta i_{fd}(s)/\Delta i_d(s)$, namely the field resistance plus metering shunt plus connecting lead and contact resistances.

4.4 Instrumentation and Connections. The measurements should be made with an instrument functionally equivalent to a transfer function analyzer, frequency response analyzer, Fourier analyzer, or digital signal analyzer. Such instruments measure the magnitudes and relative phase angles of two signals and extract only the fundamental component from any distorted waveforms. In particular, a phase-angle measurement made by a zero crossing detector will not be satisfactory for the lower frequencies.

4.4.1 Typical Test Setups. (Refer to Fig 2.) The relationships between the measured quantities and the desired variables are given in Section 5. An oscillator, sometimes an integral part of the measuring instrument, provides the test signal. This goes to a power amplifier, the output of which is connected to two terminals of the generator armature winding. The metering error of any measured transfer function should not exceed one percent at any point in the frequency range.

The power amplifier should create readily measurable signal levels for the armature and field winding voltages and currents. Test currents should be small enough to avoid temperature changes in the armature, field, or damper circuits during the test. Voltages at the armature or field winding terminals shall not exceed rated voltage levels. As a general guide, test currents would not be expected to exceed one-half of one percent of rated armature current (see 5.1).

Normal precautions to avoid overloading inputs and outputs of instruments should be observed. The impedance measured at the armature terminals at very low frequencies will be approximately twice the armature phase resistance. The maximum measured impedance will be approximately $2\ (R_2 + j\omega L_2)$, where R_2 and L_2 are the negative sequence resistance and inductance, and ω is the highest angular frequency used for the test. Both the power amplifier and the measuring instrument should be suitable for this impedance range.

4.4.2 Measurement Accuracy. Reducing or eliminating the effect of contact resistances is very important to the accuracy of the measurements, particularly on the armature winding. The armature current metering shunt should be bolted directly to the conductor in the isolated phase bus, as close to the generator terminals as possible; conducting grease should be used to enhance the contact. An instrument having differential inputs is preferred for making the measurements. Figure 3 shows the proper connection of the test leads for such a device. If an instrument with single ended inputs (common low side) is used, then the connections in Fig 4 are appropriate.

Current metering shunts are used to measure the test current supplied to the armature winding, and the induced field current. Shunt ratings should be matched to the maximum and minimum currents to appear in the respective windings. When using the test schematics in this specification, the induced field current will not exceed $\sqrt{3}\ i_s\ (I_{fdo}/i_{ao})$, where I_{fdo} is the field current required for rated armature voltage on the air-gap line, i_s is the peak value of the largest armature current used during the test, and i_{ao} is the peak value of the rated armature current; all currents are expressed in amperes. The resistance of the field winding shunt should not make the total dc resistance of the field circuit significantly greater than the field resistance at rated operating temperature.

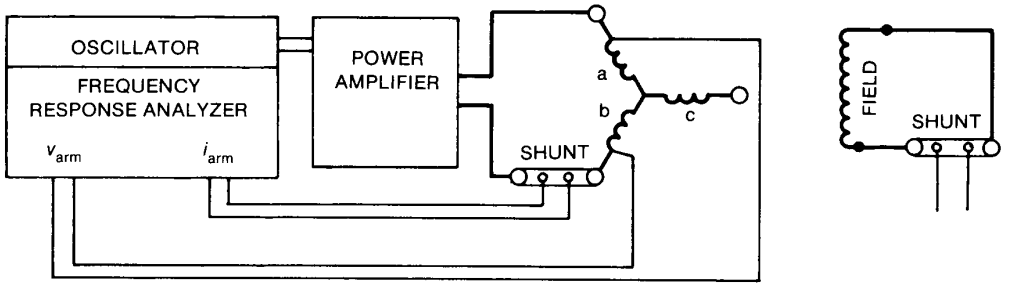

(a) MEASUREMENT OF $Z_d(s)$

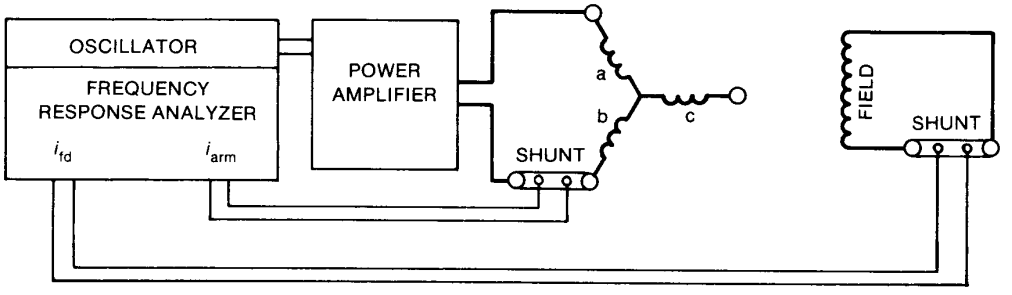

(b) MEASUREMENT OF $\Delta i_{fd}/\Delta i_{arm}$

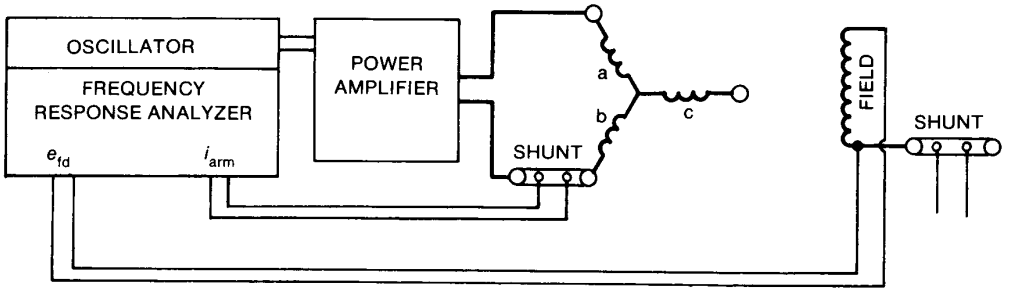

(c) MEASUREMENT OF $\Delta e_{fd}/\Delta i_{arm}$

Fig 2
Test Setup for Direct-Axis Measurements

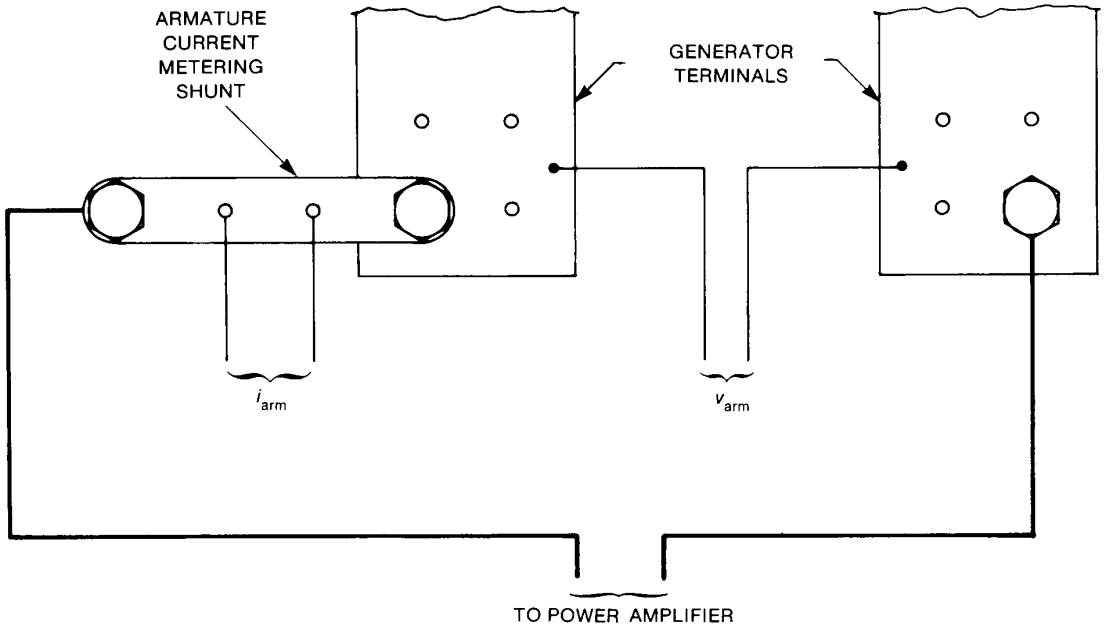

Fig 3
Connections for Differential Inputs

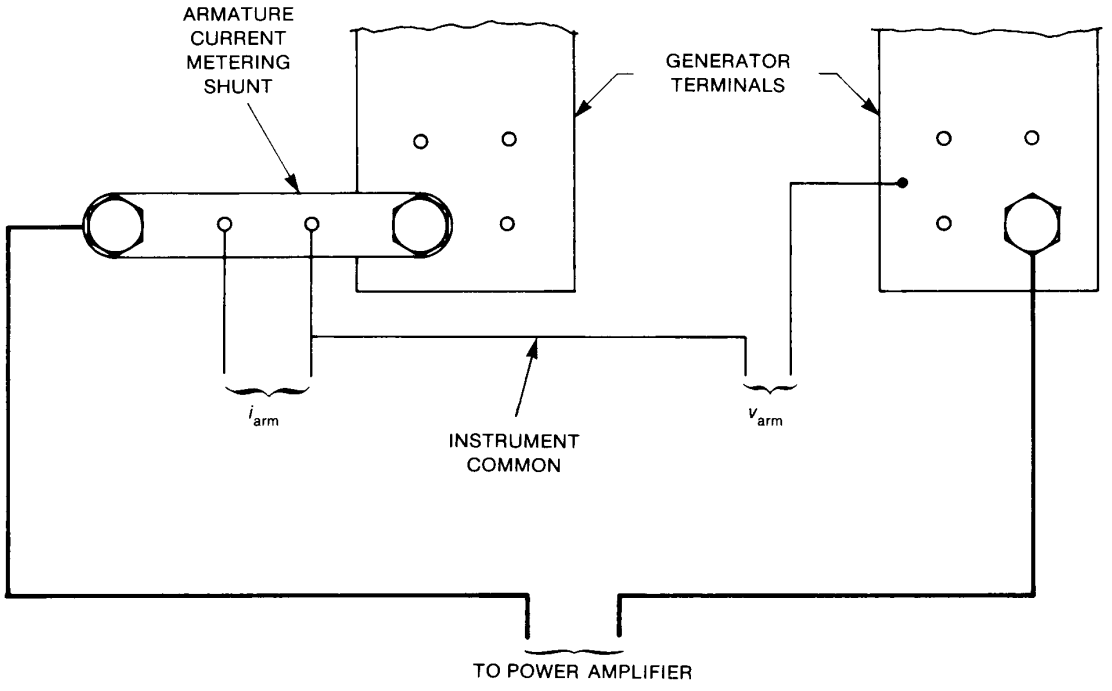

Fig 4
Connections for Single-Ended Inputs

5. Test Procedure

5.1 Machine Safety. It should be recognized that during standstill frequency response tests, the capability of the generator will be reduced with respect to its capability at normal operating conditions. Therefore, test levels of currents and voltages shall be maintained at sufficiently low levels to avoid any possible damage to either stator or rotor components. This can be achieved by limiting the maximum output of the power source to levels equal to or less than the standstill capability of the generator. The manufacturer should be consulted to identify the applicable limits.

5.2 Positioning the Rotor for *d*-Axis Tests. Temporarily connect the power amplifier as in Fig 5. Drive the amplifier with approximately 100 Hz, and measure the induced field voltage with an oscilloscope. Turn the generator rotor slowly until the induced field voltage observed on the oscilloscope is nulled. At this point, the magnetic axis of the field winding is aligned with that of the series connection of phases a and b that will be used for the direct-axis tests.

5.3 Direct-Axis Tests

5.3.1 $L_d(s)$. Referring to Fig 2(a), connect the power amplifier output to terminals a and b of the armature winding through the metering shunt. Short the field winding through a noninductive metering shunt, making solid connections to the field winding. This can be done by wrapping copper bands around the slip rings, taking care not to damage the slip rings, and bolting the shunt to the bands. In the case of a brushless exciter, it may be possible to bolt the shunt directly to the field terminals. Finally, connect the v_{arm} and i_{arm} signals to the measuring instrument so that it measures the quantity $Z_{armd}(s) = \Delta v_{arm}(s)/\Delta i_{arm}(s)$. Perform this measurement over the required frequency range. This will result in a set of test points similar to those in Fig 6. A frequency range from 0.001 to 200 Hz has been found to produce acceptable results.

Calculate the operational inductance in henrys:

$$L_d(s) = \frac{Z_d(s) - R_a}{s} \qquad \text{(Eq 8)}$$

Fig 5
Positioning the Rotor for Direct-Axis Tests

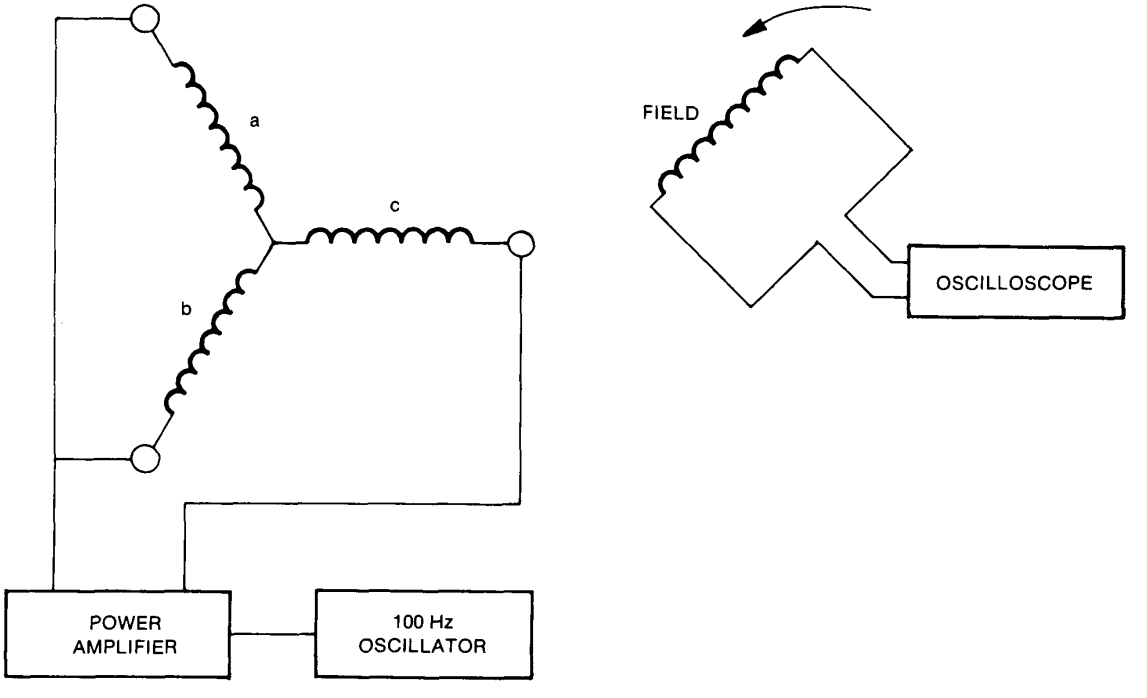

where

$$Z_d(s) = \frac{1}{2} Z_{armd}(s)$$

$$R_z = \frac{1}{2} \left\{ \lim_{s \to 0} \left[Z_{armd}(s) \right] \right\}$$

and

$$s = j\omega$$

This will result in a set of points similar to those in Fig 7, and completes the tests for the direct-axis operational inductance.

To obtain R_a, plot the real, or resistive, component of this impedance as a function of frequency, and extrapolate it to zero frequency to get the dc resistance of the two phases of the armature winding in series, $2R_a$. Care should be taken to obtain this resistance with as much accuracy and resolution as possible; otherwise, large errors in the low-frequency values for operational inductance will result. Typically, a measurement resolution of 1 part in 1000 is required at the very low frequencies. If the instrument being used cannot achieve this, satisfactory results can be obtained by spacing the measurements closer than 10 per decade and drawing a line through the scatter. Note that R_a obtained by this method should be close to the value for the armature resistance quoted by the manufacturer.

5.3.2 $sG(s)$. Now, connect the instrument to the i_{fd} and v_{arm} signal leads, Fig 2(b), and measure the transfer function $\Delta i_{fd}(s)/\Delta i_{arm}(s)$ over the required frequency range. Then, calculate

$$\frac{\Delta i_{fd}(s)}{\Delta i_d(s)} = \frac{\sqrt{3}\,\Delta i_{fd}(s)}{2\,\Delta i_{arm}(s)} \qquad \text{(Eq 9)}$$

which will lead to a plot similar to Fig 8.

5.3.3 $Z_{afo}(s)$. Finally, open the field winding by removing the field current metering shunt, and connect the i_{fd} and i_{arm} signal leads to the measuring instrument, Fig 2(c). Measure $\Delta e_{fd}/\Delta i_{arm}$ at the necessary number of frequencies, and calculate

Fig 6
***d*-Axis Impedance (Field-Shorted)**

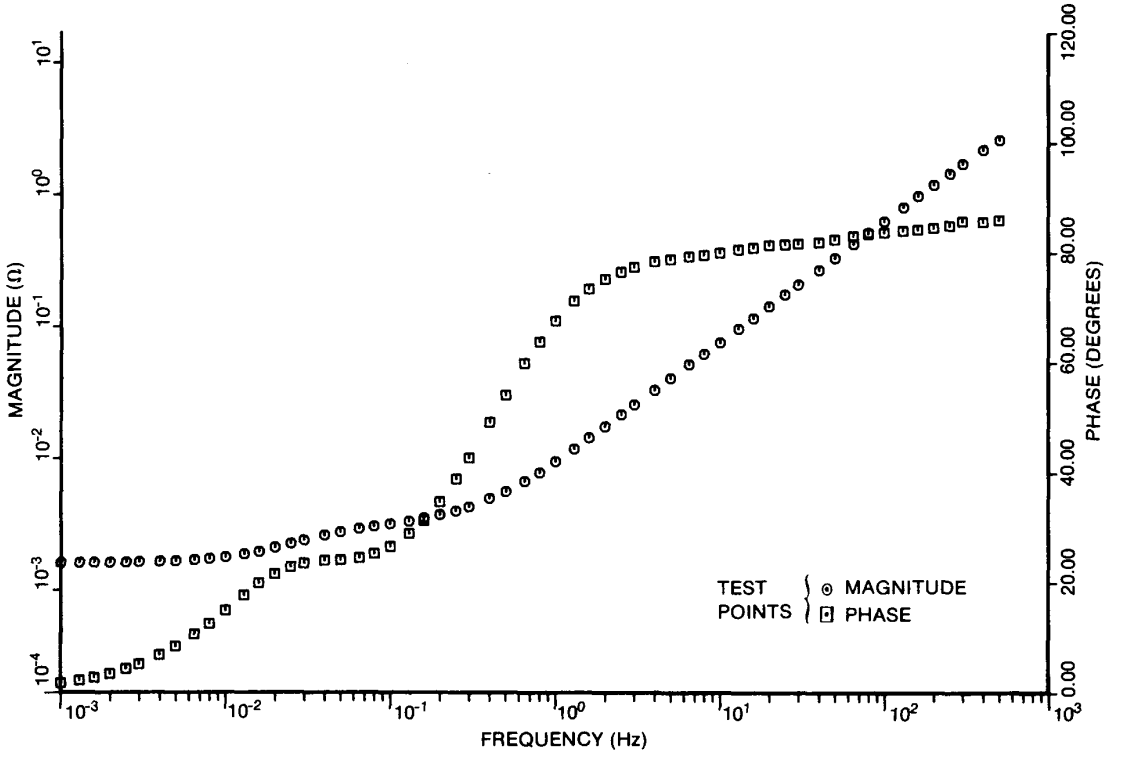

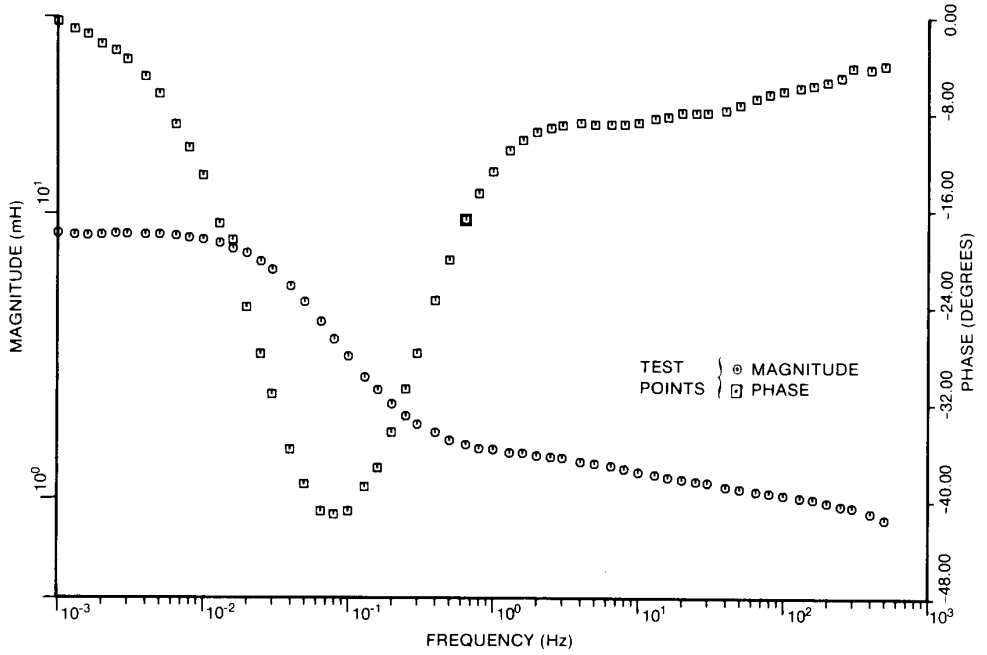

Fig 7
***d*-Axis Operational Inductance (Field-Shorted)**

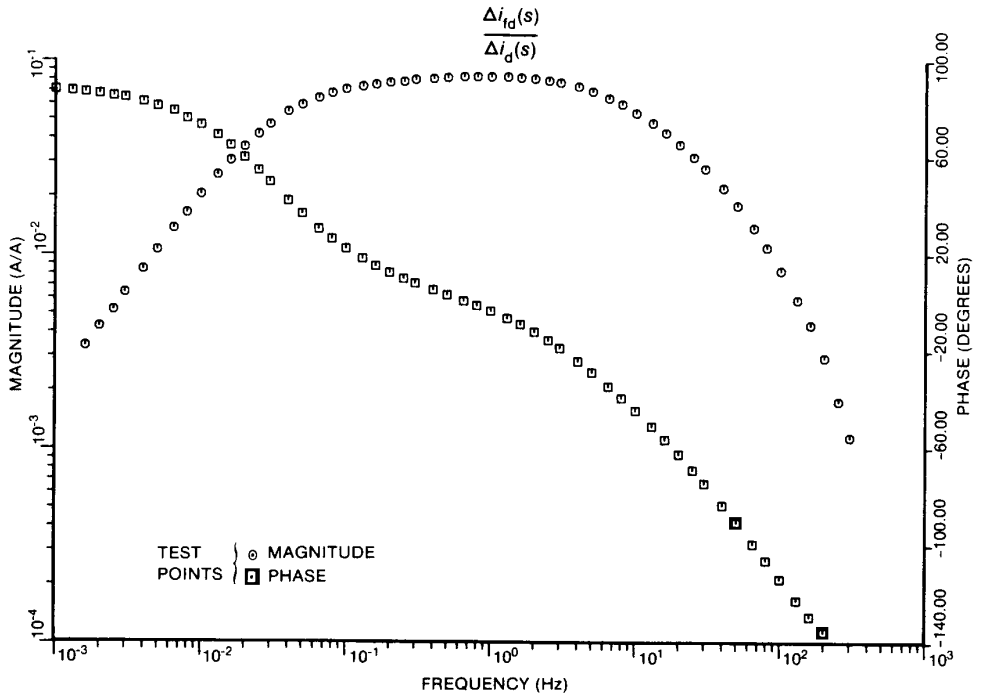

Fig 8
Standstill Armature to Field Transfer Function = $sG(s)$

$$Z_{afo}(s) = \frac{\Delta e_{fd}(s)}{\Delta i_d(s)} = \frac{\sqrt{3}}{2}\left(\frac{\Delta e_{fd}(s)}{\Delta i_{arm}(s)}\right) \quad \text{(Eq 10)}$$

When plotted, these points will be similar to Fig 9.

This completes the direct-axis tests.

5.4 Positioning the Rotor for *q*-Axis Tests. Connect the power amplifiers across phases a and b as in Fig 2 for the direct-axis measurements, remove the field current metering shunt, and set the oscillator frequency to approximately 100 Hz. Observe the induced field voltage on an oscilloscope, and turn the generator rotor slowly until a null in the induced field voltage is achieved. The rotor is now positioned for the quadrature-axis tests.

5.5 Quadrature-Axis Tests. Connect the v_{arm} and i_{arm} signal leads to the instrument to measure $Z_{armq}(s) = \Delta v_{arm}(s)/\Delta i_{arm}(s)$, as was done on the direct-axis, Fig 2(a). Measure $Z_{armq}(s)$ over the complete frequency range, and calculate

$$L_q(s) = \frac{Z_q(s) - R_a}{s} \text{ henrys} \quad \text{(Eq 11)}$$

where

$$Z_q(s) = \frac{1}{2} Z_{armq}(s)$$

and

$$R_a = \frac{1}{2}\left\{\lim_{s \to 0}\left[Z_{armq}(s)\right]\right\}$$

Note that R_a, the dc resistance of one phase of the armature winding, should be nominally the same as obtained during the direct-axis tests. However, because of the sensitivity of the results to this value, it should be obtained again using the *q*-axis data and the techniques in Section 5 in case a change in the winding temperature has altered its value since the *d*-axis tests. The plotted results for $Z_q(s)$ and $L_q(s)$ will be similar to those for the direct axis in Figs 6 and 7.

Fig 9
Standstill Armature to Field Transfer Impedance

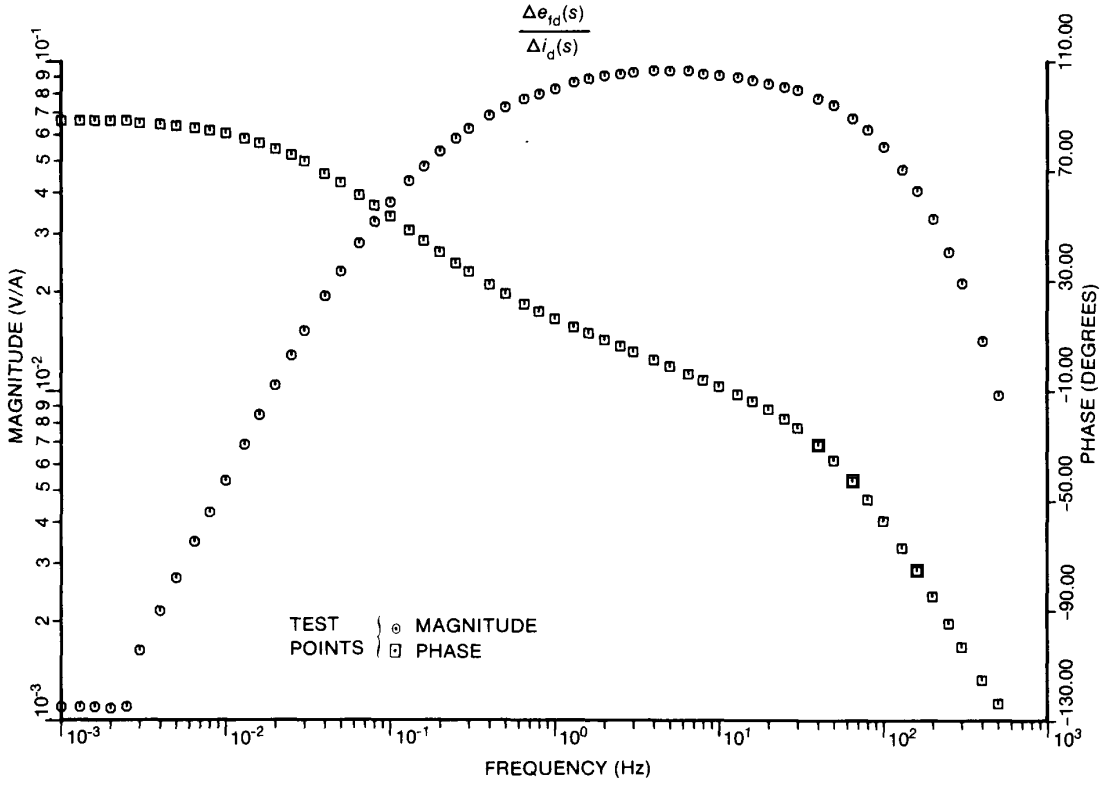

5.6 General Remarks. The preceding tests have been performed with the field aligned in a particular way for either the direct- or quadrature-axis tests. This is done to simplify the transformation of stator and field measurements of any three-phase synchronous machine to the appropriate direct- and quadrature-axis quantities. The mathematical transformations and other expressions for such d- and q-axis quantities are given in detail (see [2]). This reference also relates the measurements derived from the preceding equations (see Eq 8 through Eq 11) to a particular complexity of model. As indicated in the Appendix of this document, as well as in [2], other d- and q-axis model structures can also be chosen, of higher or lower order.

6. Nomenclature

e_d	direct-axis armature voltage
e_{fd}	field voltage
e_q	quadrature-axis armature voltage
$G(s)$	armature to field transfer function
i_{arm}	instantaneous value of armature current during test
i_{ao}	peak value of rated armature current per phase
i_d	direct-axis armature current
i_{fd}	field current
i_{fdo}	field current for rated armature voltage on the air-gap line of the open-circuit saturation curve
i_q	quadrature-axis armature current
L_{ad}	direct-axis armature to rotor mutual inductance
L_{aq}	quadrature-axis armature to rotor mutual inductance
L_{fkd}	differential leakage inductances proportional to fluxes that link one or more damper windings and the field, but that do not link the armature; $k = 1, 2, \ldots n$
L_ℓ	armature leakage inductance
L_{fd}	field winding leakage inductance
L_{kd}	direct-axis damper winding leakage inductance; $k = 1, 2 \ldots n$
L_{kq}	quadrature-axis damper winding leakage inductance; $k = 1, 2 \ldots n$
$L_d(s)$	direct-axis operational inductance
$L_q(s)$	quadrature-axis operational inductance
N_a	effective number of turns on one phase of the armature winding
N_{fd}	effective number of turns in the field winding
r_{fd}	field resistance referred to the field
R_{fd}	field resistance referred to the armature
R_{kd}	direct-axis damper winding resistance; $k = 1, 2 \ldots n$
R_{kq}	quadrature-axis damper winding resistance; $k = 1, 2, \ldots n$
s	Laplace operator
v_{arm}	voltage between two energized armature terminals during standstill frequency response tests
$Z_{afo}(s)$	standstill armature to field transfer impedance
$Z_{armd}(s)$	operational impedance measured between two armature terminals during direct-axis tests
$Z_{armq}(s)$	operational impedance measured between two armature terminals during quadrature-axis tests
$Z_d(s)$	direct-axis operational impedance
$Z_q(s)$	quadrature-axis operational impedance
Δ	small change
ω	radian frequency

NOTE: L_{fd}, L_{kd}, L_{kq}, R_{kd}, and R_{kq}: These five capitalized symbols represent rotor parameters referred to the armature; values are usually quoted in per unit on the armature impedance base.

Appendix
Obtaining Models from Standstill Test Data

(This Appendix is not a part of IEEE Std 115A-1987, IEEE Standard Procedures for Obtaining Synchronous Machine Parameters by Standstill Frequency Response Testing, but is included for information only.)

A1. Introduction

As discussed in 5.6, there are a number of possible models and procedures for reducing standstill data to model parameters. The choices of both model structure and parameter derivation techniques are independent of the measured available data. Thus, the SSFR data obtained from the tests described in Section 5 can be used to obtain a wide range of models depending upon the desires and capabilities of the user. For example, users might tend to disregard the stator to field transfer function data if accurate modeling of the field circuit was not required. It is not the intent of this document to prescribe either specific models, structures, or methods of obtaining model parameters from the SSFR data. It is recognized that since such data are only an intermediate stage in the process of model derivation, it is important to indicate to the reader how the data form a part of the overall model development process. This Appendix illustrates one possible route to the derivation of generator models from a given set of data. This is neither the only method nor is it necessarily the best.

The approach followed leads to an equivalent circuit model that is a linear lumped parameter model selected to have the same frequency, and hence, time domain characteristic as the generator. If desired, this can be converted to a model in the form of reactances and time constants by calculating these parameters from the equivalent circuit.

To avoid confusion, the calculations are done in volts, amperes, ohms, and henrys. Then, the resulting equivalent circuit elements are normalized to per unit values by dividing the base impedance or inductance of the machine, as appropriate.

A2. References

[A1] Biomedical Computer Programs, P Series, Sections 14.1 and 14.2, University of California Press, Berkeley, California, 1979.

[A2] HOOKE, R. and JEEVES, T. Direct Search Solution of Numerical and Statistical Problems, *J. Assoc. Comput.*, vol 8, no 2, Apr 1961.

[A3] RANKIN, A. W. Per Unit Impedance of Synchronous Machines, *AIEE Transactions*, vol 64, Aug 1945.

A3. General Approach

The steps for the direct axis are:

(1) Assume the best available estimate for the stator leakage inductance L_ℓ typically the value supplied by the manufacturer.

(2) $L_d(0)$ is the low-frequency limit of $L_d(s)$.

$$L_{ad} = L_d(0) - L_\ell \qquad \text{(Eq A1)}$$

NOTE: This value of L_{ad} is appropriate to the flux levels that existed during the test; in general, it will be lower than the unsaturated value associated with the air-gap line. This is discussed in Section A4.

(3) Use the $\Delta e_{fd}(s)/\Delta i_d(s)$ transfer function to find the field to armature turns ratio

$$\frac{N_{fd}}{N_a} = \left\{ \frac{1}{L_{ad}} \lim_{s \to 0} \left[\frac{1}{s} \frac{\Delta e_{fd}(s)}{\Delta i_d(s)} \right] \right\} \qquad \text{(Eq A2)}$$

(4) The field resistance, referred to the armature winding, is

$$R_{fd} = \frac{L_{ad}}{\lim_{s \to 0} \left\{ \left[\frac{1}{s} \right] \left[\frac{\Delta i_{fd}(s)}{\Delta i_d(s)} \right] \left[\frac{2}{3} \right] \left[\frac{N_{fd}}{N_a} \right] \right\}} \qquad \text{(Eq A3)}$$

NOTE: This method is used rather than direct measurement to account for the resistance of the metering shunt and connecting leads that are a part of the field circuit during the tests. However, a direct measurement of the field resistance plus the metering shunt resistance is a useful check.

(5) Define an equivalent circuit structure for the direct axis. Some possible choices are shown in Fig A1. For further background, see [2] in Section 2.

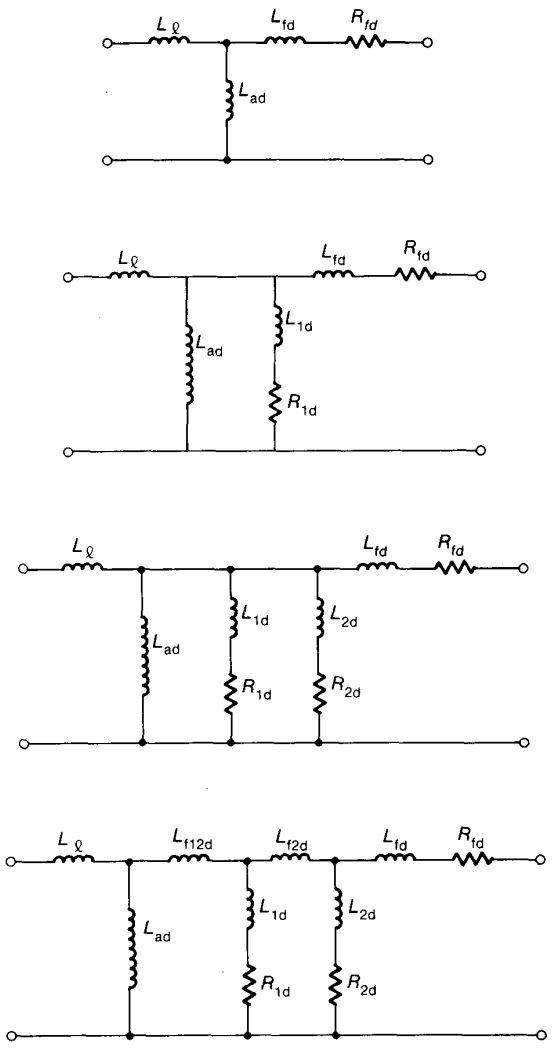

Fig A1
Direct-Axis Equivalent Circuits

(6) Use an iterative technique (see Section A5) to find values for the unknown circuit elements that produce the best fit to the two direct-axis functions $L_d(s)$ and $\frac{\Delta i_{fd}(s)}{\Delta i_d(s)}$.

NOTE: L_ℓ and R_{fd} are already determined from the previous calculations.

(7) Adjust L_{ad} calculated in (2) above to its unsaturated value L_{adu} (see Section A4).

(8) Measure the resistance of the field winding itself at the field terminals, convert it to the desired operating temperature, and refer it to the stator. For example, consider a copper winding converted to 100 °C:

$$R_{fd} \text{ at } 100\ ^\circ\text{C} = \left[\frac{234.5 + 100}{234.5 + T_f}\right]\left[r_{fd}\right]\left[\frac{3}{2}\right]\left[\frac{N_a}{N_{fd}}\right]^2 \quad \text{(Eq A4)}$$

where r_{fd} is the field resistance measured at the field terminals and T_f is the average field winding temperature in °C during the measurement. Substitute this value for R_{fd} in the equivalent circuit. For field winding materials other than copper, appropriate values of temperature coefficients (234.5 for copper) shall be used.

(9) Normalize the equivalent circuit elements to per unit values.

$$\text{(10) Base field current} = \frac{3}{2}\left(\frac{N_a}{N_{fd}}\right)\left(i_{ao}\right) \quad \text{(Eq A5)}$$

in the reciprocal per unit system.

For the quadrature axis:

(1) Assume the same value for the armature leakage inductance that was used in the d-axis.

(2) $L_q(0)$ is the low-frequency limit of $L_q(s)$.

$$L_{aq} = L_q(0) - L_\ell \quad \text{(Eq A6)}$$

Again, this value is correct for the test conditions but may be different at operating flux densities.

(3) Define an equivalent circuit structure for the quadrature axis. Some possibilities are illustrated in Fig A2.

(4) Use an iterative technique to find values for the unknown circuit elements that produce the best fit to $L_q(s)$. L_ℓ and L_{aq} are known.

(5) Convert L_{aq} to its unsaturated value (see Section A4).

(6) Normalize the equivalent circuit elements to per unit values.

A4. Magnetic Nonlinearity

It is well known that saturation reduces the inductance of iron core devices at high flux densities. However, the permeability of iron also decreases at very low flux densities. The B-H loops in Fig A3(a) illustrate this phenomenon. The apparent inductance of a coil wound on this core is proportional to the slope of the line through the tips of the appropriate B-H loops; see Fig A3(b). Thus, it is evident that the inductance of such a coil will be relatively low for a low amplitude

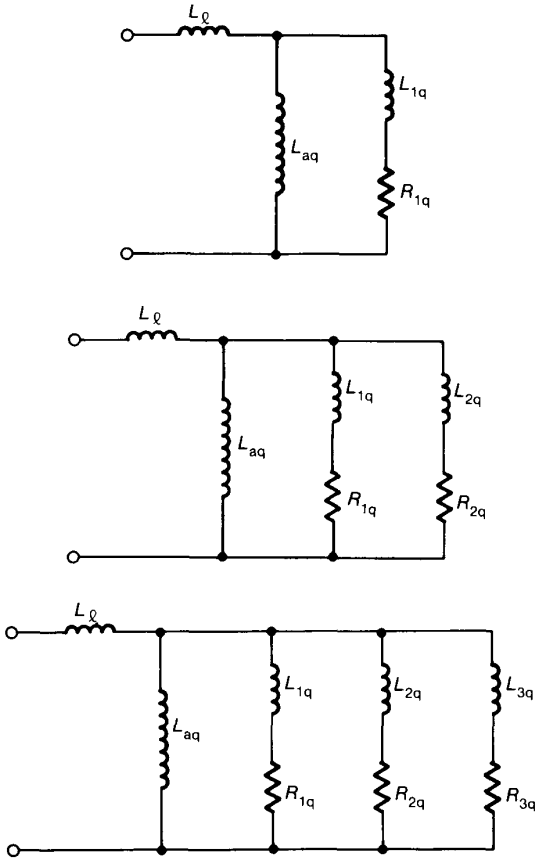

Fig A2
Quadrature-Axis Equivalent Circuits

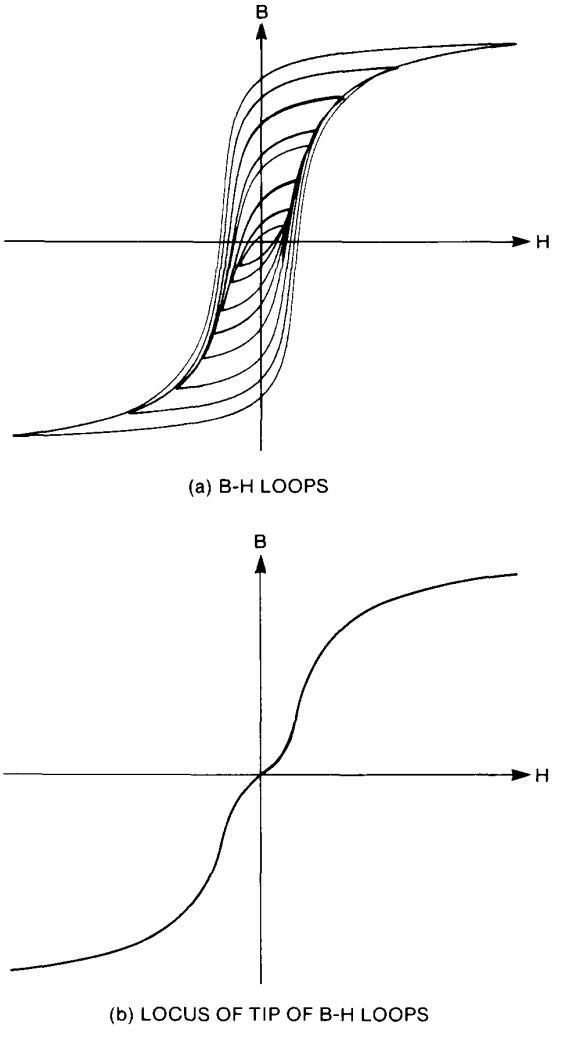

Fig A3
Magnetic Nonlinearity of Iron

cycling magnetic intensity (H). This inductance will increase to a maximum value as the amplitude of the magnetic intensity cycle gets larger; this maximum value corresponds to the air-gap line of the open-circuit saturation curve. Finally, at large amplitudes, saturation begins to limit the maximum value of flux density (B) that can be attained, and the inductance begins to decrease again.

Since standstill frequency response tests are done using very low currents (typically 40 A), compared to rated armature current, the low level iron nonlinearity cannot be ignored. In short, the values of iron-dependent inductance measured during standstill frequency response tests will be lower than unsaturated values on the air-gap line. Therefore, L_{ad} and L_{aq} in the equivalent circuits derived to match standstill test data need to be adjusted upward to achieve an unsaturated model for the machine. Generally speaking, the size of the adjustments to L_{ad} and L_{aq} will be less, if higher test currents are used.

An unsaturated value for L_{ad} in henrys can be calculated from the rated speed open-circuit saturation curve:

$$L_{adu} = \left(\frac{3}{2}\right)\left(\frac{N_a}{N_{fd}}\right)\left(\frac{V_t}{\omega I_{fd}}\right) \qquad \text{(Eq A7)}$$

where V_t and I_{fd} define a point on the air-gap line, and ω is the rotor speed in electrical radians

per second. Note that V_t is peak voltage line-to-neutral. L_{adu} is substituted for L_{ad} determined in (2) of Section A1 in the direct-axis equivalent circuit. Similarly, in the quadrature-axis equivalent circuit, L_{aq}, as determined in Section A1, must be adjusted to its unsaturated value. One possible approach is to multiply it by L_{adu}/L_{ad}, the same factor that is used in the direct axis.

A5. Curve-Fitting Procedures

Numerical values for the equivalent circuit parameters are extracted from the standstill frequency response test results by curve-fitting techniques applicable to nonlinear functions (also known as nonlinear regression analysis).

Computer programs suitable for this application typically take two forms. In one form, the user must compute only the value of a specific dependent variable—$L_q(s)$, for example—for any set of unknown parameters. Unknown parameters could be either the constants appearing in the operational form for the dependent variable; for example,

$$L_q(s) = \frac{L_q(0)\,(1 + sT'_q)\,(1 + sT''_q)}{(1 + sT'_{qo})\,(1 + sT''_{qo})} \qquad \text{(Eq A8)}$$

for the quadrature axis, or the actual equivalent circuit elements (see Fig A12, for example). The second form requires computations of both the partial derivatives of the dependent variable with respect to each of the unknown parameters and the value of the chosen independent variable. Either of these techniques might be used for the curve fits of the direct- and quadrature-axis functions. Programs that could be suitable for curve-fitting the results from standstill frequency response tests are described in [A1][3] and [A2].

The approach which has been used to produce an equivalent circuit starts in the example below with a choice of circuit form (for example, Fig A11). The stator leakage inductance L_ℓ is chosen. Then L_{ad} and R_{fd} can be calculated directly (see Eq A1 and A3). The remaining circuit elements are calculated by the following procedure:

(1) Assume some starting values for the undetermined elements.

(2) Calculate the error between the frequency response of the resulting equivalent circuit and each measured test point.

(3) Change the value of one undetermined element (for example, L_{1d}) by a small amount in one direction. If the resulting error is reduced, continue to change the value of that element in that direction until the error begins to grow instead of diminish.

(4) Repeat the process on all other undetermined elements.

(5) Reduce the size of the increment and repeat steps (3) and (4).

(6) Continue until the error between calculated points and corresponding test points cannot be reduced anymore.

A6. Example

Machine rating: 192.3 MVA, 18 kV, 60 Hz

$$\text{Armature base impedance} = \frac{(18)(18)}{192.3}$$

$$= 1.685\ \Omega$$

$$\text{Armature base inductance} = \frac{1.685}{120\,\pi}$$

$$= 4.469\ \text{mH (for 60 Hz)}$$

The manufacturer's value for armature leakage inductance L_ℓ is 0.178 pu or 0.795 mH.

Figs A4 to A7 are the four functions:

$$Z_d(s),\ \frac{\Delta e_{fd}(s)}{\Delta i_d(s)},\ \frac{\Delta i_{fd}(s)}{\Delta i_d(s)},\ Z_q(s)$$

Fig A8 is a plot of the resistive component of $Z_{armd}(s)$ at the low-frequency end of the measurements. At zero frequency, its value is $2R_a$. Accordingly, from Fig A8, $R_a = 0.001612\ \Omega$ for the example machine; therefore, the operational inductance can be calculated at each frequency. For example, at 0.13 Hz, $Z_d = 0.003370\ \underline{|30.6°}\ \Omega$. The corresponding operational inductance for this particular frequency is

$$L_d = \frac{0.003370\ \underline{|30.6°} - 0.001612}{j\,(0.13)\,(2\,\pi)}\ \text{henry}$$

$$= 0.002627\ \underline{|-36.9°}\ \text{henry} \qquad \text{(Eq A9)}$$

The unit henry ($\Omega \cdot s/\text{rad}$) is used with a complex inductance similar to what is commonly done with complex voltages and currents.

Similar calculations for each frequency at which $Z_d(s)$ was measured result in the direct-axis operational inductance plotted in Fig A9. The quadrature-axis operational inductance, $L_q(s)$,

[3] The numbers in brackets correspond to those of the references listed in Section A2 of this Appendix.

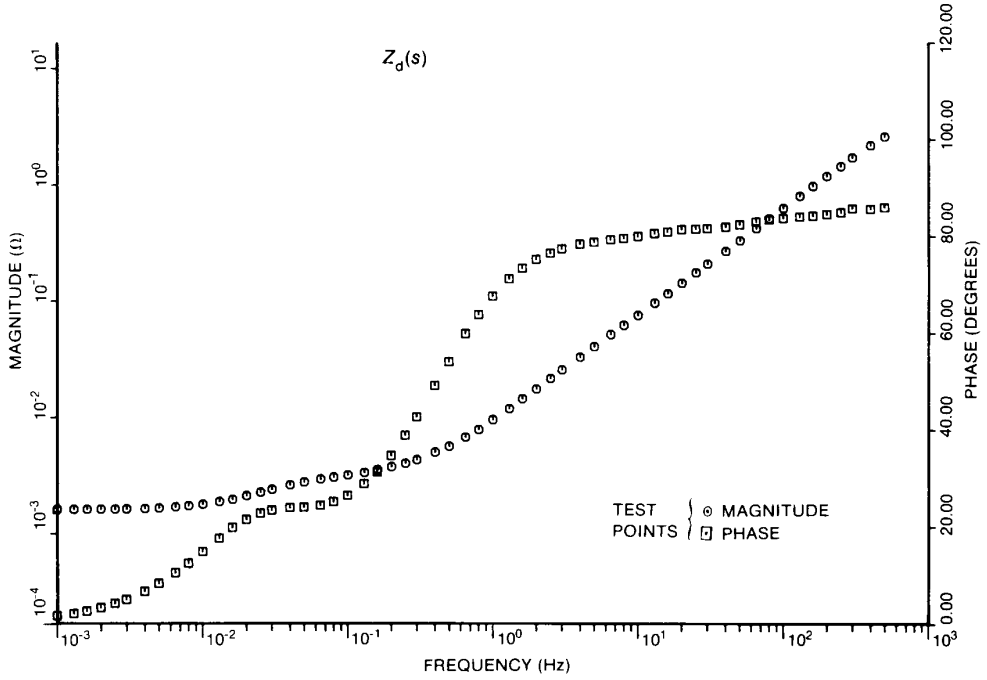

Fig A4
***d*-Axis Impedance (Field-Shorted)**

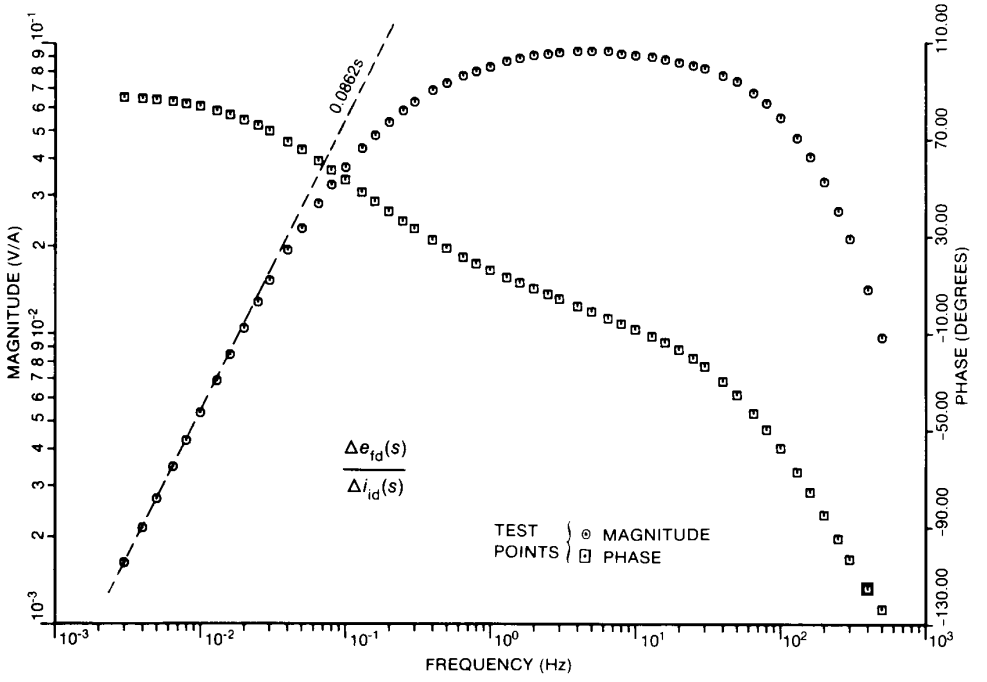

Fig A5
Standstill Armature to Field Transfer Impedance

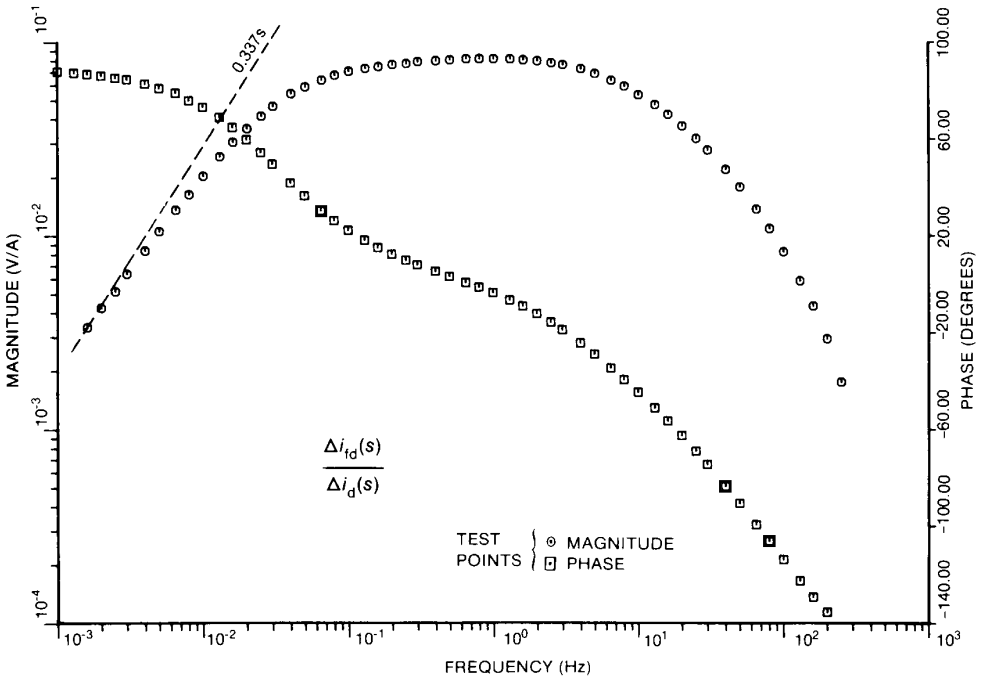

Fig A6
Standstill Armature to Field Transfer Function = $sG(s)$

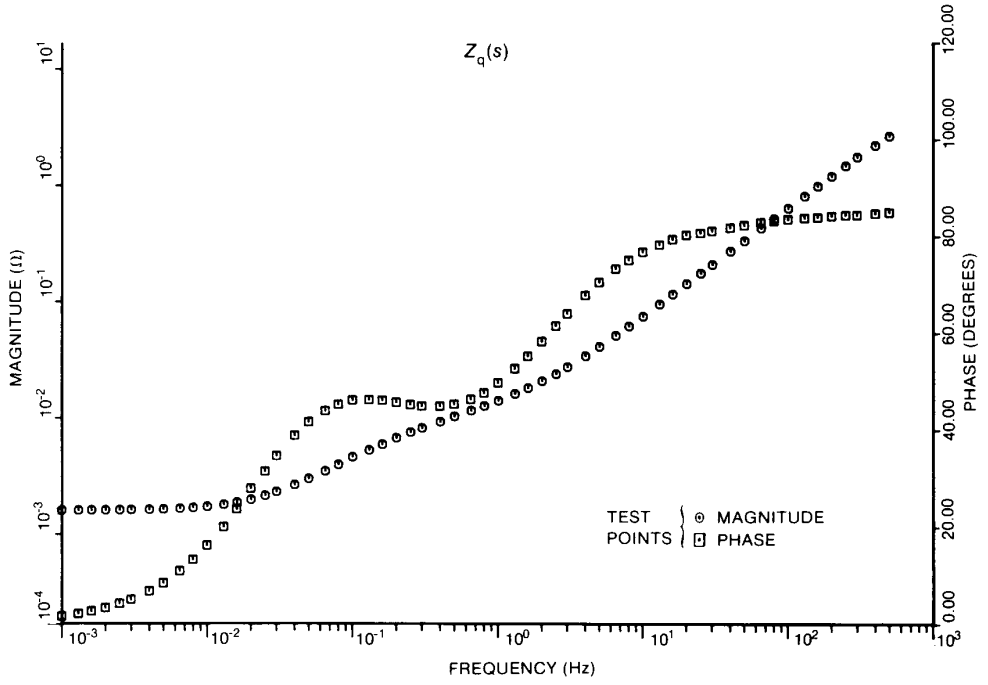

Fig A7
***q*-Axis Impedance**

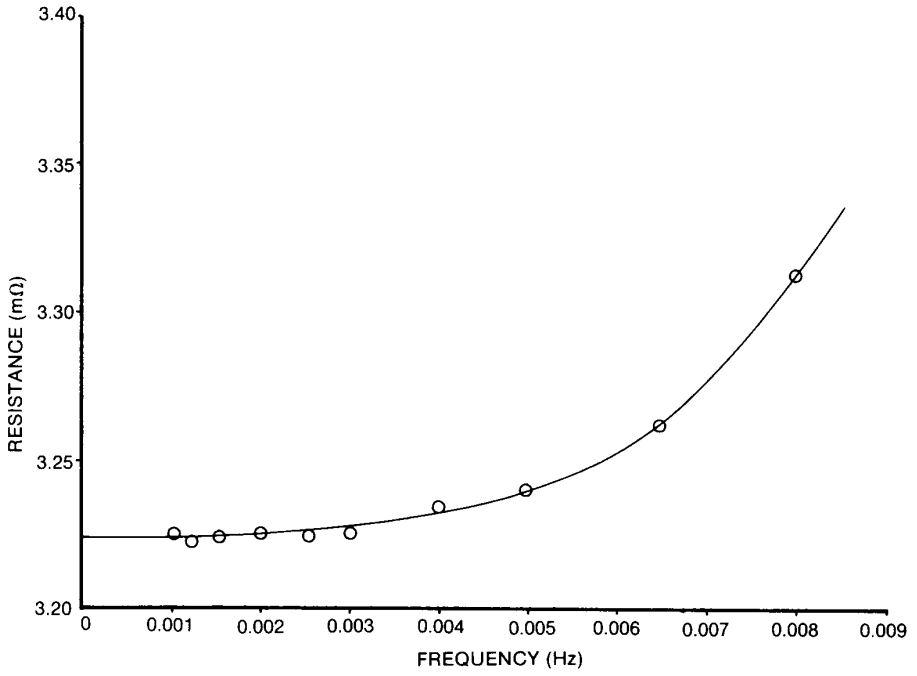

Fig A8
Resistive Component of $Z_{armd}(s)$

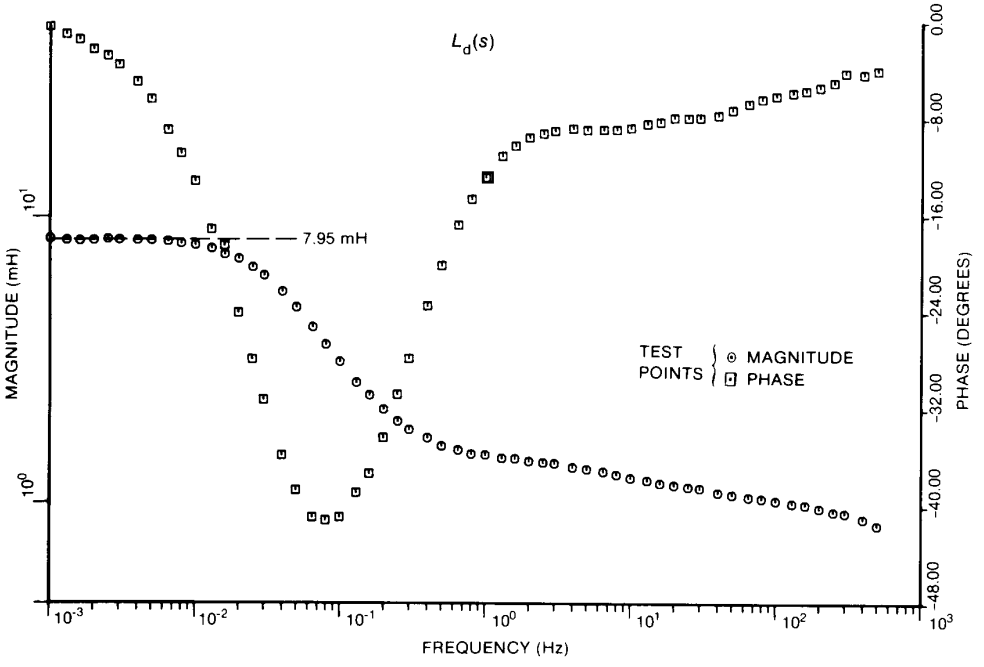

Fig A9
***d*-Axis Operational Inductance (Field-Shorted)**

plotted in Fig A10, is obtained in the same way from $Z_q(s)$.

Beginning with the direct axis and following the steps in Section A3:

(1) L_ℓ = 0.795 mH

(2) From Fig A9,

$L_d(0)$ = 1.779 pu or 7.950 mH

L_{ad} = (7.950 - 0.795) mH = 7.155 mH

(3) From Fig A5,

$$\lim_{s\to 0}\left[\frac{1}{s}\right]\left[\frac{\Delta e_{fd}(s)}{\Delta i_d(s)}\right] = 0.0862$$

Then,

$$\frac{N_{fd}}{N_a} = \frac{0.0862}{0.007155} = 12.05$$

The low-frequency limit can be obtained most accurately by fitting a function $\frac{Ks}{(1+sT)}$ to the low-frequency test points; K is the required limit.

(4) From Fig A6,

$$\lim_{s\to 0}\left[\frac{1}{s}\right]\left[\frac{\Delta i_{fd}(s)}{\Delta i_d(s)}\right] = 0.337$$

and

$$R_{fd} = \frac{0.007155}{(0.337)\left(\frac{2}{3}\right)(12.05)} = 0.002643\ \Omega$$

during the standstill tests.

(5) The equivalent circuit structure in Fig A11 will be used for the direct axis.

From previous calculations,

L_ℓ = 0.795 mH

L_{ad} = 7.155 mH

R_{fd} = 0.002643 Ω

(6) The iterative curve fit procedure described at the end of Section A5 yields the following values for the unknown elements:

L_{f12d} = 0.267 mH

L_{f2d} = 0 mH

Fig A10
***q*-Axis Operational Inductance**

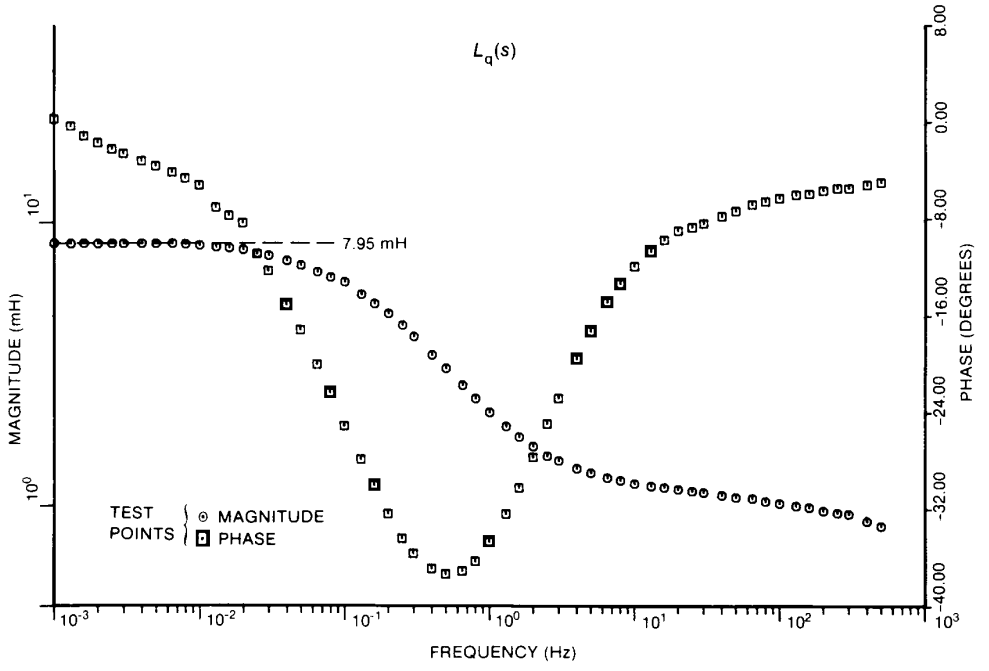

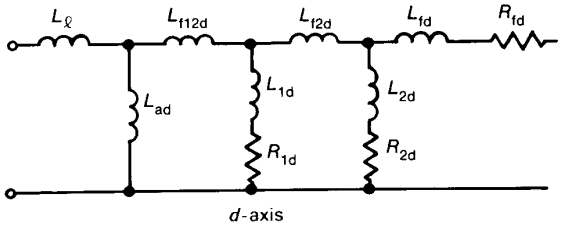

Fig A11
Assumed Direct-Axis Equivalent Circuit

L_{1d} = 0 mH

R_{1d} = 0.0263 Ω

L_{2d} = 2.282 mH

R_{2d} = 0.006574 Ω

L_{fd} = 0.726 mH

(7) At rated armature voltage on the air-gap line of the open-circuit saturation curve, I_{fdo} = 590 A.

$$L_{adu} = \left[\frac{3}{2}\right]\left[\frac{1}{12.05}\right]\left[\frac{18\,000\sqrt{2}}{(\sqrt{3})(120\pi)(590)}\right] = 8.225 \text{ mH}$$

Substitute 8.225 mH for the previous value of 7.155 mH in the direct-axis equivalent circuit.

(8) The measured field winding resistance was 0.2045 Ω at 20 °C. At 100 °C,

$$R_{fd} = \left[\frac{234.5+100}{234.5+20}\right]\left[0.2045\right]\left[\frac{3}{2}\right]\left[\frac{1}{12.05}\right]^2$$

$$= 0.002777\ \Omega$$

(9) Converting to per unit values,

$$L_\ell = \frac{0.795}{4.469} = 0.178 \text{ pu}$$

$$L_{adu} = \frac{8.225}{4.469} = 1.840 \text{ pu}$$

$$L_{f12d} = \frac{0.267}{4.469} = 0.060 \text{ pu}$$

L_{1d} = 0

$$R_{1d} = \frac{0.0263}{1.685} = 0.0156 \text{ pu}$$

L_{f2d} = 0

$$L_{2d} = \frac{2.282}{4.469} = 0.511 \text{ pu}$$

$$R_{2d} = \frac{0.006574}{1.685} = 0.00390 \text{ pu}$$

$$L_{fd} = \frac{0.726}{4.469} = 0.162 \text{ pu}$$

$$R_{fd} = \frac{0.002777}{1.685} = 0.00165 \text{ pu}$$

(10) Base armature current

$$= \frac{192.3 \text{ MVA}}{18\sqrt{3} \text{ kV}} = 6.168 \text{ kA rms}$$

Base field current will be defined according to Rankin's "x_{ad} bases" (see [A3]).

$$\text{Base field current} = \left[\frac{3}{2}\right]\left[\frac{1}{12.05}\right]\left[6168\sqrt{2}\right]$$

$$= 1086 \text{ A}$$

Note the similarity between this and another common approach also described in [A3]:

$$\text{Base field current} = I_{fdo}\, x_{adu}$$

$$= 590 \times 1.84$$

$$= 1086 \text{ A}$$

$$\text{Base field impedance} = \frac{\text{rated VA}}{(\text{base field current})^2}$$

$$= \frac{192.3 \times 10^6}{(1086)^2}$$

$$= 163.05\ \Omega$$

At 100 °C, the field resistance is

$$r_{fd} = \left(\frac{334.5}{254.5}\right)\left(0.2045\right) = 0.2688\ \Omega$$

or

$$R_{fd} = \frac{0.2688}{163.05} = 0.00165 \text{ pu}$$

The quadrature axis is considered next.

(1) L_ℓ = 0.795 mH

(2) From Fig A10,

$L_q(0)$ = 7.950 mH

L_{aq} = (7.950 - 0.795) mH = 7.155 mH

NOTE: This machine is somewhat atypical; usually, $L_{ad} > L_{aq}$.

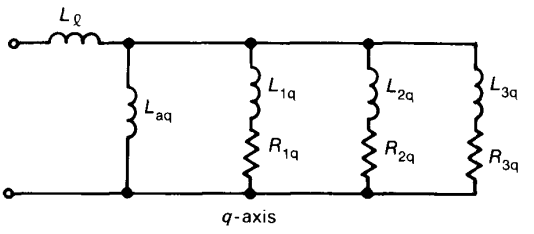

Fig A12
Assumed Quadrature-Axis Equivalent Circuit

(3) The quadrature-axis equivalent circuit structure is shown in Fig A12.

L_l and L_{aq} are known.

(4) An iterative procedure, identical to that described above, fitted to the quadrature-axis operational inductance produced:

L_{1q} = 6.045 mH

R_{1q} = 0.01355 Ω

L_{2q} = 0.735 mH

R_{2q} = 0.01525 Ω

L_{3q} = 0.453 mH

R_{3q} = 0.1578 Ω

$$L_{aqu} = L_{aq}\left(\frac{8.225}{7.155}\right)$$

$$= 7.155\left(\frac{8.225}{7.155}\right)$$

= 8.225 mH

(5) Converting to per unit values,

$$L_\ell = \frac{0.795}{4.469} = 0.178 \text{ pu}$$

$$L_{aqu} = \frac{8.225}{4.469} = 1.840 \text{ pu}$$

$$L_{1q} = \frac{6.045}{4.469} = 1.353 \text{ pu}$$

$$R_{1q} = \frac{0.01355}{1.685} = 0.00804 \text{ pu}$$

$$L_{2q} = \frac{0.735}{4.469} = 0.164 \text{ pu}$$

$$R_{2q} = \frac{0.01525}{1.685} = 0.00905 \text{ pu}$$

$$L_{3q} = \frac{0.453}{4.469} = 0.101 \text{ pu}$$

$$R_{3q} = \frac{0.1578}{1.685} = 0.0936 \text{ pu}$$

These values constitute an unsaturated quadrature-axis model for the machine.

A7. Concluding Comments

In the preceding example, the test data were fitted to the most complex models shown in Figs A1 and A2. Furthermore, as a result of the calculations, all elements of the models were assigned specific values. It should be emphasized that if simpler models with a smaller number of elements are chosen, a completely new set of calculations is required in order to fit the elements of the simpler models to the data. In most cases a less exact fit will be obtained, but the values calculated for the simpler model structure may often be quite adequate for the stability requirements of the user.